Acta Crystallographica Section F
Structural Biology and Crystallization Communications
ISSN 1744-3091

A C-terminal disulfide bond in the copper-containing amine oxidase from pea seedlings violates the twofold symmetry of the molecular dimer

Anthony P. Duff,[a]‡ Eric M. Shepard,[b] David B. Langley,[a] David M. Dooley,[b] Hans C. Freeman[a] and J. Mitchell Guss[a]*

[a]School of Molecular and Microbial Biosciences, University of Sydney, NSW 2006, Australia, and [b]Department of Chemistry and Biochemistry, Montana State University, Bozeman, MT 59717, USA

‡ Present address: ANSTO, Private Mail Bag, Menai, NSW 2234, Australia

Correspondence e-mail: m.guss@mmb.usyd.edu.au

Received 21 August 2006
Accepted 19 October 2006

PDB Reference: PSAO, 1w2z, r1w2zsf.

The structure of a newly crystallized form of the copper-dependent amine oxidase from pea seedlings has been refined at a resolution of 2.2 Å to a final *R* factor of 0.181. The structure (form II) was originally discovered during a study of xenon binding to copper-dependent amine oxidases as a probe for dioxygen-binding sites [Duff *et al.* (2004), *J. Mol. Biol.* **344**, 599–607]. The form II crystals belong to space group $P2_1$, with two dimers in the asymmetric unit. The overall structure is very similar to the crystals of form I in space group $P2_12_12_1$ with a dimer in the asymmetric unit [Kumar *et al.* (1996), *Structure*, **4**, 943–955]. In form I the last three residues (644–647) observable in the two subunits were apparently splayed apart. It was noted that the absence of a disulfide bond between the Cys647 residues of the two subunits was inconsistent with chemical evidence for the absence of free sulfhydryl groups. In both of the crystallographically independent dimers of form II the two subunits are clearly joined by a disulfide bridge between the C-terminal cysteine residues. This is only possible if the two polypeptide chains in the dimer adopt different conformations near the C-terminus so that the twofold symmetry is lost. A proline residue (645) two residues before the cysteine has a *cis* conformation in one chain and a *trans* conformation in the other. As a result, the disulfide bond lies more than 5 Å from the twofold axis. The loss of local twofold symmetry in form II can be explained by intermolecular contacts, which provide an asymmetric environment.

1. Introduction

Copper amine oxidases (CuAOs; Dove & Klinman, 2001) are ubiquitous enzymes that catalyse the oxidative deamination of a primary amine to an aldehyde according to the overall reaction

$$R\mathrm{CH_2NH_3^+} + \mathrm{O_2} + \mathrm{H_2O} \rightarrow R\mathrm{CHO} + \mathrm{NH_4^+} + \mathrm{HOOH}.$$

The active site includes a Cu^{II} atom and an organic cofactor, which is 2,4,5-trihydroxyphenylalanine quinone (TPQ) in all structurally characterized CuAOs. TPQ is produced spontaneously by the oxidation of a conserved tyrosine residue in the presence of molecular oxygen and the Cu cofactor. Catalysis then proceeds *via* a ping-pong mechanism, with the TPQ alternating between the oxidized form and a two-electron-reduced NH_2-substituted aminoquinol (TPQ_{red}) according to the half-reactions

$$R\mathrm{CH_2NH_2} + \mathrm{TPQ} \rightarrow R\mathrm{CHO} + \mathrm{TPQ_{red}},$$
$$\mathrm{TPQ_{red}} + \mathrm{O_2} + \mathrm{H_2O} \rightarrow \mathrm{TPQ} + \mathrm{NH_3} + \mathrm{HOOH}.$$

TPQ-containing CuAOs have been found in a wide range of organisms from bacteria to humans, where they appear to perform a multitude of biological roles. In microorganisms, amine oxidases generally play a nutritional role in the utilization of primary amines as the sole source of nitrogen. In plants, they have been implicated in wound healing. In mammals, functions such as detoxification have been identified and some CuAOs are known to be tissue-specific. Since the physiological function of amine oxidases in higher organ-

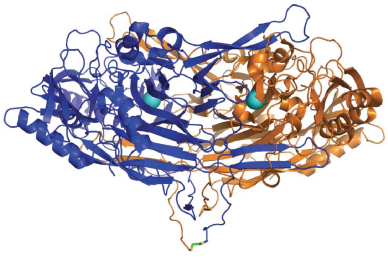

Table 1
Crystal data and refinement statistics for form II PSAO.

Values in parentheses are for the highest resolution shell.

Crystallization conditions	20% PEG 3350, 0.28 *M* KI pH 7.2
Space group	$P2_1$
Unit-cell parameters (Å, °)	a = 89.5, b = 196.3, c = 89.7, α = 90, β = 107.5, γ = 90
Solvent content (%)	54
Matthews coefficient (Å^3 Da^{-1})	2.7
No. of subunits per ASU	4
Data-collection temperature (K)	100
Wavelength (Å)	1.54
Resolution range (Å)	30–2.24
No. unique reflections	133957
Completeness (%)	99.8 (98.9)
Redundancy	4.75 (4.7)
$R_{\rm merge}$†	0.07 (0.17)
No. of non-H atoms refined	21682
Average B value (Å^2)	20
$R_{\rm cryst}$‡	0.181
$R_{\rm free}$§	0.224
ESU based on maximum likelihood¶ (Å)	0.140
Ramachandran outliers (%)	0.0
Ramachandran favoured (%)	97.3
R.m.s.d. from standard geometry	
Bond lengths (Å)	0.012
Bond angles (°)	1.3
PDB code	1w2z

† $R_{\rm merge} = \sum_h \sum_i |I_i - \langle I \rangle| / \sum_h \sum_i I_i$. ‡ $R_{\rm cryst} = \sum_h |F_h({\rm obs}) - F_h({\rm calc})| / \sum_h F_h({\rm obs})$. § $R_{\rm free} = R_{\rm cryst}$ for approximately 5% of the data (7082 reflections) not used during refinement. ¶ ESU, estimated uncertainty from *REFMAC* refinement (Murshudov & Dodson, 1997).

isms is frequently associated with the breakdown or transformation of biologically active amines, these enzymes may act as regulators of physiological amine concentrations and therefore may participate in numerous biological processes (Cohen, 1998).

PSAO is one of seven structurally characterized CuAOs (Fig. 1). The others are *Escherichia coli* amine oxidase (ECAO; Parsons *et al.*, 1995), *Arthrobacter globiformis* amine oxidase (AGAO; Wilce *et al.*, 1997), *Hansenula polymorpha* amine oxidase (HPAO; Li *et al.*, 1998), *Pichia pastoris* lysyl oxidase (PPLO; Duff *et al.*, 2003), bovine serum amine oxidase (BSAO; Lunelli *et al.*, 2005) and the human vascular adhesion protein (VAP-1; Airenne *et al.*, 2005; Jakobsson *et al.*, 2005). All are homodimers of similar size and topology. In each subunit, the N-terminal domains D2 and D3 pack against a large core formed by the two symmetry-related D4 domains. Two long β-hairpin arms protrude from each D4 domain and embrace the other D4 domain, contributing to a large buried subunit interface. One active site is buried deeply in each D4 domain and is accessed by substrates *via* a channel from the surface of the enzyme. The residues that line the channel belong to the D2, D3 and D4 domains of one subunit and to the tip of one of the β-hairpin arms of the symmetry-related subunit. A large solvent-filled 'lake' lies between the two D4 domains. In all the structures, the lake is connected with the external solvent *via* openings on and around the dimer twofold axis. ECAO alone has an additional N-terminal D1 domain in each subunit. If the rest of the enzyme molecule is described as the cap of a mushroom, the adjoining D1 domains represent the stalk (Parsons *et al.*, 1995).

The existence of form II of PSAO was mentioned briefly in a previous publication, the main emphasis of which was on the use of xenon to probe potential oxygen-binding sites in CuAOs (Duff *et al.*, 2004). The description of the PSAO structure was limited to the Xe-binding sites. We now describe the structure of form II of PSAO and compare it with form I (Kumar *et al.*, 1996).

2. Materials and methods

2.1. Enzyme purification and crystallography

PSAO was extracted from pea seedlings (8 kg) and was purified as described previously (McGuirl *et al.*, 1994). A freshly purified sample was crystallized by hanging-drop vapour diffusion at 293 K (the reservoir contained 20% PEG 3350, 0.28 *M* KI; the 4 µl drops contained 2 µl of 21.6 mg ml^{-1} protein in 0.1 *M* K_2PO_4/$KHPO_4$ pH 7.2, 1 µl 0.1 *M* K_2PO_4/$KHPO_4$ pH 7.5 and 1 µl reservoir solution). A crystal was cryoprotected by soaking for 5 min in 5 µl 0.2 *M* KI, 25% PEG 3350 and 15% glycerol under 30 µl of paraffin in a sitting-drop depression slide. The crystal was exposed to xenon gas as described previously (Duff *et al.*, 2004) and was then cryocooled rapidly in liquid nitrogen. Data were also recorded for native crystals in the absence of xenon gas but under otherwise identical conditions. The best native crystals diffracted to a lower resolution ($d_{\rm min} > 2.6$ Å) than the Xe-pressurized crystals. The native data were only used to identify the Xe-binding sites (see below).

Diffraction data (Table 1) were recorded from a crystal at 100 K in a stream of cold nitrogen gas using a MAR Research 345 mm imaging plate with X-rays generated by a Rigaku RU-200 generator with a Cu anode (λ = 1.5418 Å) and Osmic optics. The data were integrated using *DENZO* and *SCALEPACK* (Otwinowski & Minor, 1997). The structure was solved by molecular replacement using *MOLREP* (Vagin & Teplyakov, 1997), with all protein atoms of a dimer from the form I crystal structure of PSAO (PDB code 1ksi; Kumar *et al.*, 1996) as the search model. Refinement was carried out using *REFMAC* (Murshudov *et al.*, 1997). Tight main-chain and medium side-chain NCS restraints between the four monomers in the asymmetric unit

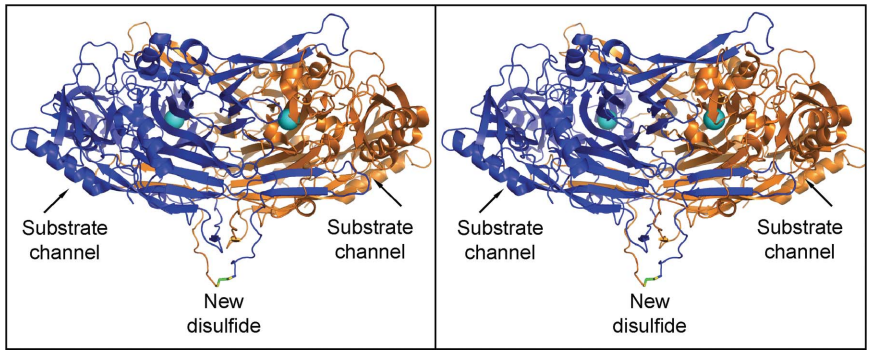

Figure 1
Stereoview of a dimeric PSAO molecule as observed in the form II crystals. Chain *A* is coloured blue and chain *B* is coloured orange. The active-site Cu atoms (shown as cyan spheres) are buried deep in the core of the protein. In the view shown, the active site is accessed *via* channels on the lower left and right. The C-termini of the two subunits meet at the bottom of the enzyme. The newly observed disulfide bridge between Cys*A*647 and Cys*B*647 is shown as a green bond.

were applied at residues 6–639, with the exception of residues affected by crystal packing (49, 87, 148, 469, 472–747, 537 and 573). For the C-terminal residues 640–647, NCS restraints were applied separately between chains *A* and *C* and between chains *B* and *D*. Two Xe atoms per subunit and 176 I^- ions were modelled and refined. Real and anomalous electron-density peaks that were absent in maps calculated with the native PSAO data but present in maps calculated with the Xe-PSAO data identified the Xe sites. Other real and anomalous peaks in maps calculated with both the Xe-PSAO and native PSAO data identified I^- sites. The occupancy of each Xe and I^- site was determined in *CNS* (Brünger *et al.*, 1998) by iteratively refining the occupancy and *B* factor until convergence. Structures were validated using *WHATCHECK* (Vriend, 1990) and *MOLPROBITY* (Lovell *et al.*, 2003).

3. Results and discussion

3.1. Structure of PSAO in crystal form II

Coincidentally, the crystal data and structure-refinement statistics for the form II and form I crystal structures of PSAO are remarkably similar; each structure was refined at a resolution of 2.2 Å and reached a final *R* value of 0.181. The model in each case includes residues 6–647. Table 1 contains details of the data and refinement statistics for crystal form II.

In form II, the asymmetric unit contains four chains (*A*, *B*, *C*, *D*) assembled as two dimers (*AB* and *CD*). Amino-acid residues 6–647 and carbohydrate residues attached to Asn131 and Asn558 have been modelled in each chain. The electron density was not sufficiently well resolved to model residues 1–5 or 648–649 in any chain. Up to residue 643, the dimers *AB* and *CD* have nearly perfect local twofold symmetry (see below).

The active-site Cu atoms and TPQ cofactors are well resolved in all four subunits. The TPQ cofactors are in the 'off-Cu' conformation. The electron density for their O2 and O5 atoms implies that the quinone rings have two coplanar conformations related by a 180° rotation about χ_2 (Fig. 2). Similar observations were previously reported for PSAO form I and for other CuAOs (Murray *et al.*, 1999).

In addition, the model of form II contains eight Xe atoms, 176 I^- ions and 581 water molecules. Two Xe atoms are bound internally in each monomer. Xe atoms related by NCS were assigned identical occupancies (0.78 for one set of four and 0.21 for the other set of four Xe atoms). I^- sites were refined without NCS and have occupancies ranging from 0.22 to 1.00. All I^- sites are located on the protein surface or in the central lake. The presence of a large number of I^- ions apparently has no significant effect on the backbone structure of the protein, as indicated by a comparison with the form I structure. However, many surface side chains adopt different conformations as a result of I^- binding in form II or differences between intermolecular contacts in forms I and II.

3.2. Dimer asymmetry at the C-termini

The only significant and important difference between the structures of forms I and II of PSAO involves the last four observable residues before the C-terminus of each chain: namely, Trp644, Pro645, Gly646 and Cys647. In form I, these residues, with the exception of the side chain of Trp644, conform approximately to the local twofold symmetry of the dimer. Pro645 has a *trans* peptide and the S atoms of the two Cys647 residues are separated by 13.6 Å. The *B* factors of Gly646 and Cys647 are very high (62–75 $Å^2$). The side chain of Trp644 differs between the chains in both crystal forms. The side chain of Trp*A*644 is well resolved on the dimer axis, making it impossible to model both side chains symmetrically while maintaining acceptable stereochemistry.

In form II, residues 644–647 do not obey the local twofold symmetry in either of the two crystallographically independent dimers. In the *AB* dimer the C-terminus of chain *A* is different from that of chain *B* and in the *CD* dimer the C-terminus of chain *C* is different from that of chain *D*. Chain *A* is very similar to chain *C* and chain *B* is very similar to chain *D*. These observations were confirmed by means of OMIT maps in which the respective residues were omitted from the calculation of structure factors prior to several rounds of further refinement. Although the omit electron density was weak and not completely continuous, an unambiguous interpretation could be made (Fig. 3).

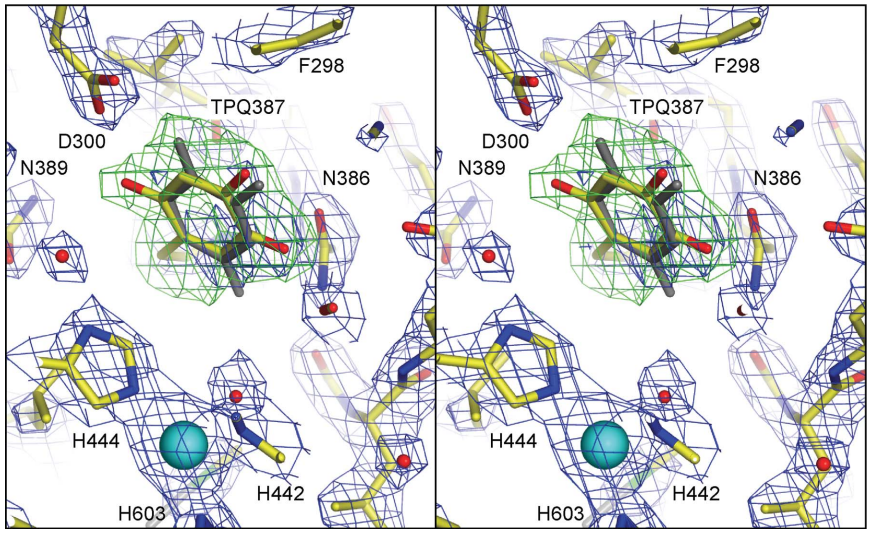

Figure 2
Stereoview of an active site in PSAO, highlighting the TPQ cofactor. TPQ is shown in two conformations. The second conformer, coloured grey, is flipped 180° about χ_2. The OMIT density (green, contoured at 3.5 times the root-mean-square electron density) is the average of the densities in the four crystallographically independent subunits. The $2F_o - F_c$ density (blue, contoured at 1.5 times the root-mean-square electron density) was calculated with phases from the final model.

At Trp*A*644 and Trp*B*644 (and at the corresponding residues in chains *C* and *D*), the backbone groups are related by the local twofold symmetry but the side chains clearly have different conformations (Fig. 3). The side chain of Trp*A*644 (*C*644) crosses the local twofold axis, while that of Trp*B*644 (*D*644) points away from this axis. The deviation of the backbone from local twofold symmetry begins at the next residue, Pro645. The peptide group of Pro*A*645 (*C*645) is *cis*, while that of Pro*B*645 (*D*645) is *trans*. The electron density at Gly*A*646 (*C*646) and Gly*B*646 (*D*646) is weak but above the noise level. At Cys*A*647 (*C*647) and Cys*B*647 (*D*647), the backbone is not resolved in the electron density, but the side chains are clearly visible and indicate the presence of disulfide bonds (*A*647)–S–S–(*B*647) and (*C*647)–S–S–(*D*647). The *B* factors for S^{γ} atoms of the four Cys residues are 51–53 Å^2.

We can reconcile the observation of asymmetry in form II with the apparent lack of asymmetry in form I of PSAO as follows. Both of the conformations observed for residues 644–647 in each chain are compatible with the crystal packing in form I, but not in form II (Fig. 4). In form I, the C-termini are present as a disordered mixture of the two conformations. This is indicated by the very high *B* factors for Gly646 and Cys647 where, we now deduce, each conformation is present with only half occupancy. To test this hypothesis, we followed the suggestion of a reviewer and re-refined the original form I structure after replacing the free Cys residues with the two disulfide bridges found in the form II structure. Neither of the residuals *R* and $R_{\rm free}$ changed significantly (data not shown). In other words, the data for form I at 2.2 Å resolution can be fitted equally well by the chemically incorrect form I structure and by the chemically correct model derived from form II. A probable reason is that the positions of the Cys S atoms in the disulfide bridge are not very different from the positions of the free Cys S atoms in the original structure. Thus, while the original model was chemically incorrect in that it lacked a disulfide link, it nevertheless modelled the electron density reasonably well at 2.2 Å resolution. The packing in form II selects an

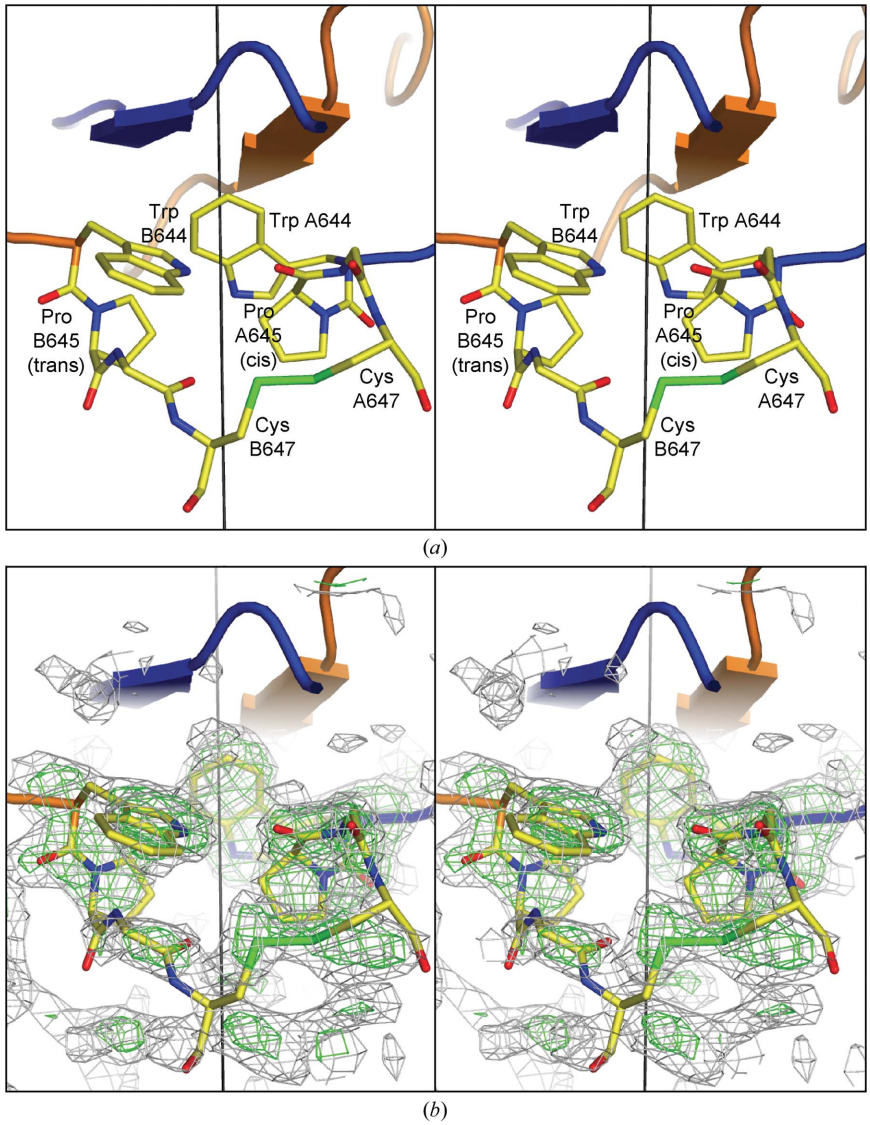

Figure 3
Stereoviews of the C-terminal residues and the newly identified disulfide bond. (*a*) The residues which violate the local twofold symmetry are labelled. The side chain of Trp644 has different orientations in the two chains. Pro645 is *cis* in chain *A* and *trans* in chain *B*. The disulfide bond linking Cys*A*647 and Cys*B*647 is shown in green. (*b*) OMIT density (green, contoured at 3.5 times the root-mean-square electron density; grey, contoured at 2.0 times the root-mean-square electron density) is averaged over the two crystallographically independent dimers. The S atoms of Cys*A*647 and Cys*B*647 are associated with strong electron density.

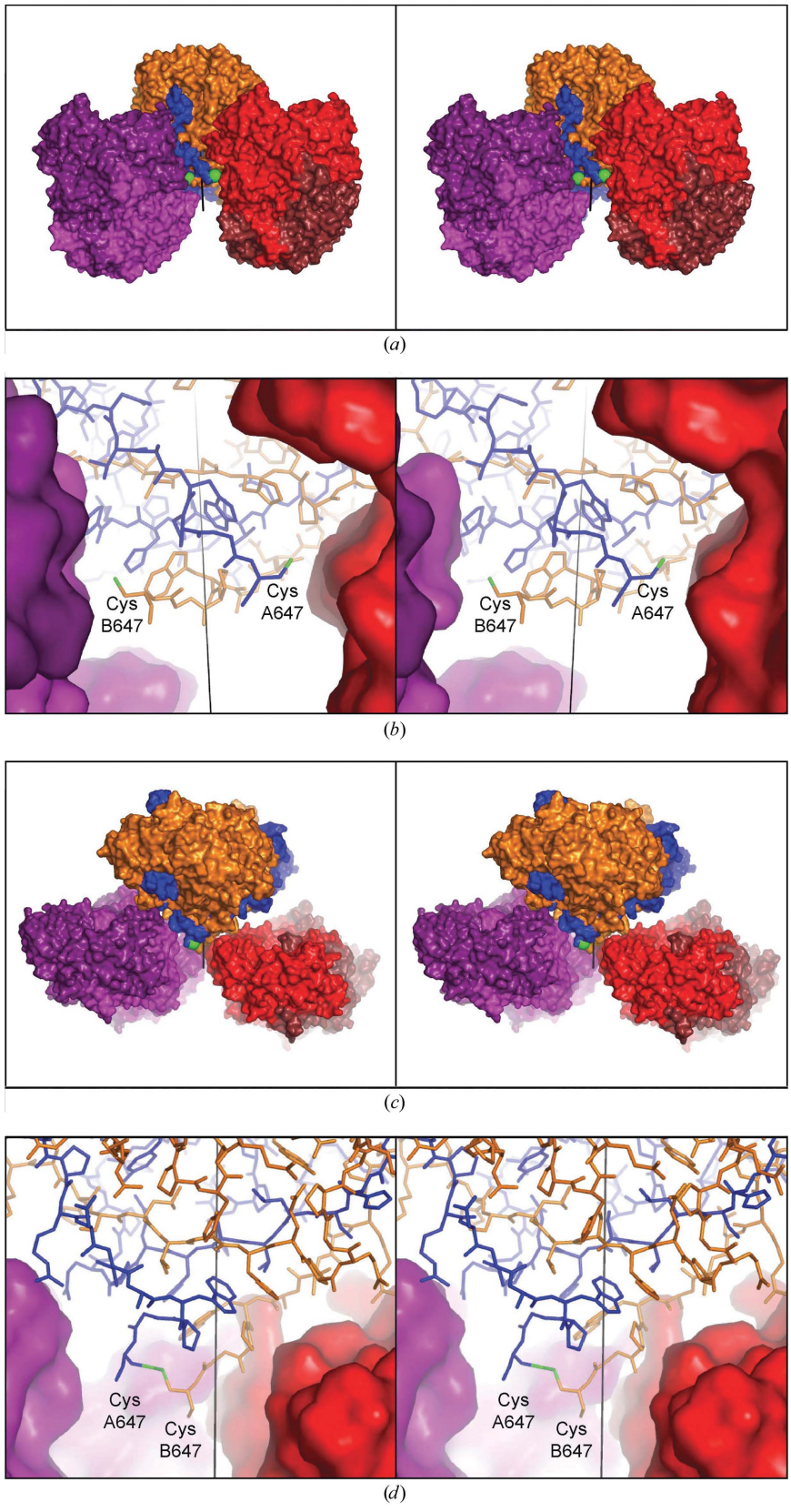

Figure 4
Stereoviews of the packing of the C-termini in the two crystal forms of PSAO. In each structure, chain *A* is shown in blue and chain *B* in orange. The Cys647 S^{γ} atoms are shown as large green spheres in (*a*) and (*c*). The local twofold dimer axis is shown as a black line. The neighbouring molecules that lie close to the C-termini are coloured red/dark red in one dimer and purple/dark purple in the other. (*a*) Space-filling representation of the packing in PSAO form I. (*b*) Enlargement of the region around the C-terminus of PSAO form I, showing how both conformations can be accommodated. (*c*) Space-filling representation of the packing in PSAO form II. (*d*) Enlargement of the region around the C-termini of PSAO form II, showing how the packing prevents the two polypeptide chains from adopting a symmetrical arrangement.

ordered arrangement in which the two chains of the dimer have different conformations. The fact that the electron density is only weak indicates that the formation of a disulfide bond does not restrict the mobility of the other C-terminal residues significantly. The presence of a disulfide, whether observed (form II) or not (form I), is consistent with biochemical data showing that the PSAO holoenzyme has no free sulfhydryl groups (Kumar *et al.*, 1996).

4. Conclusion

The disulfide bond observed in form II of PSAO and inferred indirectly in form I of PSAO is likely to be present in other CuAOs with an appropriately located Cys residue. Crystallographically, disulfide bonds involving a cysteine residue near the C-terminus have been observed in VAP-1 (Airenne *et al.*, 2005; Jakobsson *et al.*, 2005) and PPLO (Duff *et al.*, 2003). In VAP-1, the chains of the dimer are linked by a disulfide bond between Cys*A*748 and Cys*B*748. The crystal structure of PPLO has two disulfide bonds per dimer, but in this case they link a residue close to the C-terminus (Cys756) to one near the N-terminus (Cys45) of the same chain.

Disulfide bonds similar to that in PSAO may also be present in AGAO and HPAO. Like PSAO, AGAO and HPAO have a cysteine as the third-last residue of the wild-type sequence. For AGAO, Wilce *et al.* (1997) cited an unpublished observation that the holoenzyme has no free sulfhydryl groups, implying that Cys*A*315, Cys*B*315, Cys*A*636 and Cys*B*636 are disulfide-bonded. However, the absence of observable electron density implied that such a disulfide is in a flexible part of the molecule. It is possible that HPAO similarly contains disordered disulfide bonds involving the residues Cys689 and Cys690. ECAO has no cysteine residues and hence no disulfide bonds. The purpose of the disulfide bond (where it exists) remains to be rationalized.

This work was supported by the Australian Research Council (DP0557353 to JMG, HCF and DMD) and by the National Institutes of Health, USA (GM27659 to DMD).

References

Airenne, T. T., Nymalm, Y., Kidron, H., Smith, D. J., Pihlavisto, M., Salmi, M., Jalkanen, S., Johnson, M. S. & Salminen, T. A. (2005). *Protein Sci.* **14**, 1964–1974.

Brünger, A. T., Adams, P. D., Clore, G. M., DeLano, W. L., Gros, P., Grosse-Kunstleve, R. W., Jiang, J.-S., Kuszewski, J., Nilges, M., Pannu, N. S., Read, R. J., Rice, L. M., Simonson, T. & Warren, G. L. (1998). *Acta Cryst.* D**54**, 905–921.

Cohen, S. S. (1998). *A Guide to Polyamines.* Oxford University Press.

Dove, J. E. & Klinman, J. P. (2001). *Adv. Protein Chem.* **58**, 141–174.

Duff, A. P., Cohen, A. E., Ellis, P. J., Kuchar, J. A., Langley, D. B., Shepard, E. M., Dooley, D. M., Freeman, H. C. & Guss, J. M. (2003). *Biochemistry*, **42**, 15148–15157.

Duff, A. P., Trambaiolo, D. M., Cohen, A. E., Ellis, P. J., Juda, G. A., Shepard, E. M., Langley, D. B., Dooley, D. M., Freeman, H. C. & Guss, J. M. (2004). *J. Mol. Biol.* **344**, 599–607.

Jakobsson, E., Nilsson, J., Kallstrom, U., Ogg, D. & Kleywegt, G. J. (2005). *Acta Cryst.* F**61**, 274–278.

Kumar, V., Dooley, D. M., Freeman, H. C., Guss, J. M., Harvey, I., McGuirl, M. A., Wilce, M. C. J. & Zubak, V. M. (1996). *Structure*, **4**, 943–955.

Li, R., Klinman, J. P. & Mathews, F. S. (1998). *Structure*, **6**, 293–307.

Lovell, S. C., Davis, I. W., Arendall, W. B. III, de Bakker, P. I., Word, J. M., Prisant, M. G., Richardson, J. S. & Richardson, D. C. (2003). *Proteins*, **50**, 437–450.

Lunelli, M., Di Paolo, M. L., Biadene, M., Calderone, V., Battistutta, R., Scarpa, M., Rigo, A. & Zanotti, G. (2005). *J. Mol. Biol.* **346**, 991–1004.

McGuirl, M. A., McCahon, C. D., McKeown, K. A. & Dooley, D. M. (1994). *Plant Physiol.* **106**, 1205–1211.

Murray, J. M., Saysell, C. G., Wilmot, C. M., Tambyrajah, W. S., Jaeger, J., Knowles, P. F., Phillips, S. E. & McPherson, M. J. (1999). *Biochemistry*, **38**, 8217–8227.

Murshudov, G. N. & Dodson, E. J. (1997). *CCP4 Newsl.* **33**, 31–39.

Murshudov, G. N., Vagin, A. A. & Dodson, E. J. (1997). *Acta Cryst.* D**53**, 240–255.

Otwinowski, Z. & Minor, W. (1997). *Methods Enzymol.* **276**, 307–326.

Parsons, M. R., Convery, M. A., Wilmot, C. M., Yadav, K. D., Blakeley, V., Corner, A. S., Phillips, S. E., McPherson, M. J. & Knowles, P. F. (1995). *Structure*, **3**, 1171–1184.

Vagin, A. A. & Teplyakov, A. (1997). *J. Appl. Cryst.* **30**, 1022–1025.

Vriend, G. (1990). *J. Mol. Graph.* **8**, 52–56.

Wilce, M. C. J., Dooley, D. M., Freeman, H. C., Guss, J. M., Matsunami, H., McIntire, W. S., Ruggiero, C. E., Tanizawa, K. & Yamaguchi, H. (1997). *Biochemistry*, **36**, 16116–16133.